Volume 20, No 3 | International Journal of Radiation Research, July 2022

Identifying features and severity of 2019 coronavirus disease (COVID-19) on admission based on thoracic computer tomography

Z. Mo, Q. Zhang, X.W. Luo*, Y. Zhang*, T. Qin, Y.Z. Zhu

[1]*Department of Radiology, The 901st Hospital of the Joint Logistics Support Force of PLA, Heifei 230031, People Republic of China*

[2]*Department of Radiology, Wuhan Taikang Tongji Hospital, Wuhan 430050, People Republic of China*

► ***Original article***

Corresponding authors:
Prof. Yu Zhang and Xiang-wei Luo,
E-mail:
zhangyu105fsk@163.com

Received: August 2021
Final revised: September 2021
Accepted: February 2022

Int. J. Radiat. Res., July 2022; 20(3): 579-585

DOI: 10.52547/ijrr.20.3.9

Keywords: *2019 coronavirus disease, pneumonia, Tomography, X-ray compute.*

ABSTRACT

Background: To investigate the computer tomography (CT) features of 2019 coronavirus disease (COVID-19)-related pneumonia and its value for identifying severity. ***Materials and Methods***: Seventy-three patients with COVID-19 were divided into severe and nonsevere groups. CT signs were divided into two states: presence and absence; involvement range was divided into four grades; and affected lobes were divided into two states: ≥3 lobes and < 3 lobes; laboratory indices were divided into two states: normal and abnormal; co-occurrence of signs was divided into three states: ground-glass opacity (GGO) plus consolidation, only GGO, or only consolidation. The numbers of patients were respectively recorded. Statistical analysis was performed through the χ2 test, followed by multivariate logistic regression analysis. ***Results***: Some indicators differed, including pure GGO (p<0.001), GGO with focal consolidation (p=0.009), patchy consolidation (p=0.004), sheeted consolidation (p<0.001), fibrotic appearance (p=0.020), involvement grade (p<0.001), affected lobes (p=0.027), pleural effusion (p=0.001), subpleural line (p=0.015), crazy paving signs (p<0.001), halo signs (p=0.020), thickened bronchial walls (p<0.001), air bronchi signs (p=0.003), lesions in mid/inner zone (p<0.001), liver function (p=0.044), interleukin-6 (p<0.001), c-reactive protein (p<0.001), lymphocyte count (p<0.001), and age (p=0.036). Pure GGO (OR:30.711, HR:1.292~729.882, p=0.034) and involvement grade (OR:0.017, HR:0.001~0.342, p=0.008) were independent risk factors. ***Conclusion***: On admission, CT signs of COVID-19-related pneumonia were diverse but characteristic, and some CT findings may be potential warning factors for severity, while a lack of GGO and extensive pneumonia may be independent risk factors.

INTRODUCTION

Since December 2019, unknown viral pneumonia of clustered incidence has occurred in the region of Huanan Seafood Market, Wuhan, China. Before long, the pathogen was identified by Chinese scientists as a novel coronavirus. Subsequently, 2019 novel coronavirus (2019-nCoV) has been called, and the novel coronavirus disease was referred to as "2019 coronavirus disease (COVID-19)" by the World Health Organization (WHO), instead of calling it "Severe acute respiratory syndrome coronavirus 2 (SARS-CoV-2)" [1-3]. Under the Chinese government's efforts, despite huge economic losses, most patients were residents of Hubei Province, and the number of newly confirmed cases nationwide has dropped significantly [4,5]. However, recently, the epidemic has rebounded in some parts of the world, and controlling and preventing the epidemic has become a difficult long-term task. 2019-nCoV is related to the coronaviruses that cause SARS and Middle East respiratory syndrome (MERS) and is closely related to coronaviruses carried by bats; however, the intermediate hosts have still not been clearly identified [1,6]. At present, based on some studies, it may be prudent to determine whether Wuhan, China, was the only origin of global transmission of the novel virus [4,5,7].

Due to the increasing number of worldwide cases, the WHO announced that the epidemic was a "global pandemic", and countries not only needed to tackle domestic epidemics but also faced the risk of internationally imported cases. Identify COVID-19 as soon as possible is a challenging task at the first visit to a hospital.

However, as the gold standard for diagnosis, although viral nucleic acid detection has strong specificity, its sensitivity is poor and it is slow, and it may produce false negative results. In earlier studies, some scholars believed that positive detection by lung CT may be possible earlier than via clinical manifestations and concurrent nucleic acid tests [8]. CT is highly sensitive compared to the initial reverse transcription-polymerase chain reaction (RT–PCR)

[DOI: 10.52547/ijrr.20.3.9]

testing, and CT may be a very important screening method for COVID-19 [1, 9]. Although how to implement CT properly is controversial, CT may be one of the most convenient and useful alternatives in resource-constrained districts with outbreaks [10]. Therefore, to identify COVID-19 and accurately determine severity, it is necessary to identify the CT signs of pulmonary lesions, which is beneficial to diagnose and isolate high-risk patients early, assess the severity of pneumonia in a timely manner and improve the hospital infection control process. In fact, in some studies, different CT findings with varying course of disease or in patients with mild or severe disease were be described [1, 11], and chest CT score based on the extent of lobar involvement and lesion volume-level quantitative features based on artificial intelligence (AI) system to predict prognosis were be reported [12, 13]. However, to data, there were few systematic discussions on the progression to severe disease based on the prediction of multiple CT signs at admission. To accomplish this, we analyzed the CT features and differences between 73 cases of severe and non-severe COVID-19 in patients on admission and explored weather some CT signs may predict the trend of severe disease.

MATERIALS AND METHODS

The study was conducted in accordance with the Declaration of Helsinki, and the protocol was approved by the Ethics Committee of 901st Hospital of the Joint Logistic Support Force of People's Liberation Army (No. 2020030102). Informed consent for this retrospective study was waived.

Patients' sources

The clinic information and CT images of 73 patients with COVID-19 at the 901st Hospital of the Joint Logistics Support Force of PLA and Wuhan Taikang Tongji Hospital were collected from February 2020 to March 2020. All patients were confirmed by clinical and 2019-nCoV nucleic acid RT–PCR testing (BGI, China). Patients with pneumonia, caused by other common bacterial and viral pathogens, were excluded. The severity of disease in all patients was determined in accordance with the community-acquired pneumonia guidelines of the North American thoracic society [14]. All patients underwent thin section CT scans at the time of initial admission. All patients had no previous major organ damage, such as damage to the heart, liver, kidneys or lungs.

Image acquisition

All patients were performed with a 256-section scanner (Revolution 256 CT, GE, USA) with plain scan and iterative reconstruction technique. The CT parameters were as follows: scan type, helical; tube voltage 120 kV; automatic tube current (80 mA-475 mA); collimation, 0.625 mm; beam pitch, 1; scan range covering the whole lung. Reconstruction was performed using lung high-resolution/standard mode with a thickness of 0.625 mm and interval of 0.625 mm. CT images were observed by using the mediastinal window and lung window.

Image analysis

All CT images were independently reviewed by three radiologists with more than 5 years of clinical experience in respiratory radiology. Any disagreements were resolved by discussion and consensus. All radiologists were blinded to the clinical conditions of the patients. All CT features were defined based on the article [8,15,16], and CT features were retrospect on the basis of the following aspects: consolidation and consolidation types (acinar/nodular consolidation, patchy consolidation, sheeted consolidation); ground-glass opacity (GGO) and its types (pure GGO, GGO with fine reticulation, GGO with focal consolidation); fibrotic appearance (presenting ≥1 of the following signs: tractional bronchiectasis, streak shadow with visceral pleural adhesions, interlobar fissure contraction); thickened bronchial walls; parallel sign (when the long axis of lesion was parallel to the pleural surface, it was defined as a parallel sign); halo sign and reversed halo sign; subpleural line sign; crazy paving sign; pleural effusion; distribution of lesions (the region of lung in the plane of the lobe and segmental bronchi was considered to be the inner zone of lung, the region of lung in the plane of segmental bronchi was considered to be the middle zone of lung, and the regions of lung in the plane of segmental distal bronchi, costal subpleural and near the interlobar fissure region were considered to be the outer zones of the lung); number of involved lobes; grade of lung involvement range (based on the article [15, 16], it was simplified into four grades, Ⅰ grade: 1% ~ 25%, Ⅱ grade: 26% ~ 50%, Ⅲ grade: 51% ~ 75%, Ⅳ grade: ≥76%). All signs and cases were recorded individually.

Statistical methods

Based on the grouping of patients with severe and non-severe disease, CT signs were divided into two states: presence and absence. Pulmonary lesions were classified into three states: GGO plus consolidation, only GGO, or only consolidation. The involvement range of the lung was divided into four grades, the number lung lobes involved was divided into two states: ≥3 lobes and < 3 lobes, and laboratory indices were divided into two states: normal and abnormal. The number of patients was recorded for each category, and the lists were then established. Finally, SPSS 25.0 software was used to conduct statistical analysis with the $\chi 2$ test, and multivariate logistic regression analysis was

[DOI: 10.52547/ijrr.20.3.9]

conducted for the CT signs with significant differences. P <0.05 was considered statistically significant.

RESULTS

Clinical characteristics

36 were males and 37 were females, the ages were 24 to 94 years, the average age was 62.32±13.637 years, all were Chinese Han nationality, 64 patients had a cough, 55 patients had a fever, and 24 patients had dyspnea. 21 patients had severe disease. On admission, 72 patients were tested for liver function, of which 22 patients (30.56%) had abnormal liver function, 71 patients were tested for interleukin-6 (IL-6,), of which 26 patients (36.62%) had elevated IL-6 levels, 69 patients were tested for c -reactive protein levels, of which 19 patients (27.54%) had elevated c-reactive protein levels, all the patients underwent routine blood tests, of which 22 patients (30.14%) had decreased lymphocyte counts.

CT features of pulmonary lesions

Multiple lesions were observed in all patients. GGO was noted in 72 patients (72/73, 98.63%), including 52 patients (52/73, 71.23%) with pure GGO (figure 1), 65 patients (65/73, 89.04%) with GGO plus fine reticulation (figures 1, 2), and 38 patients (38/73, 52.05%) with GGO plus focal consolidation (figures 3, 4, 5). Consolidation was present in 50 patients (50/73, 68.49%) (figures 3 and 4), including 36 patients with acinar/nodule consolidation (36/73, 49.32%) (figure 3), 36 patients with patchy consolidation (36/73, 49.32%) (figure 3a), and 8 patients with sheeted consolidation (8/73, 10.96%). A fibrotic appearance was observed in 40 patients (40/73, 54.79%). A halo sign was observed in 4 patients (4/73, 5.48%) (figure 3b), reversed halo sign in 6 patients (6/73, 8. 22%) (figure 5b), crazy paving sign in 20 patients (20/73, 27.40%) (figure 4), thickened bronchial walls in 28 patients (28/73, 38.36%), air bronchi sign in 28 patients (28/73,38.36%), subpleural line sign in 22 patients (22/73,30.14%) (figure 1b), parallel sign in 54 patients (54/73, 73.97%) (figures 1, 2, 5), and small amount of pleural effusion in 4 patients (4/73, 5.48%). Lesions in 73 patients (73/73, 100%) were located in the mid/outer zone of the lung, and 39 patients (39/73, 53.42%) also had lesions in the mid/ inner zone of the lung. More than three lobes were involved in 62 patients (62/73, 84.93%). The involvement range of lung tissue was grade Ⅰ in 29 patients (29/73, 39.73%), grade Ⅱ in 23 patients (23/73, 31.51%), grade Ⅲ in 12 patients (12/73, 16.44%), and grade Ⅳ in 9 patients (9/73, 12.33%). All patients had no cavities, tree-in-bud signs in the lungs, or enlarged lymph nodes in the hilum and mediastinum.

Statistical analysis of clinical characteristics and CT features of COVID-19

Some clinical indicators and CT features with significant differences were demonstrated between the nonsevere and severe groups (table 1). Multivariate logistic regression analysis was performed on the indicators with significant differences, including pure GGO, sheeted consolidation, crazy paving sign, thickened bronchial walls, grade of involvement area and lesions in mid/ inner zone of the lung. Among them, pure GGO and grade of involvement were independent risk factors on CT for patients with severe disease (table 2).

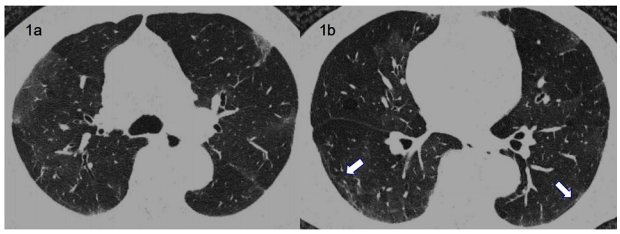

Figure 1. A 74-year-old female patient with nonsevere COVID-19. A CT scan showed multiple patchy pure GGO in the subpleural area of the right upper lobe and GGO with fine reticulation in the subpleural area of the left upper lobe. plus the long axis was parallel to the pleural surface **(1a)**; the subpleural line sign was demonstrated in both inferior lobes **(1b)**.

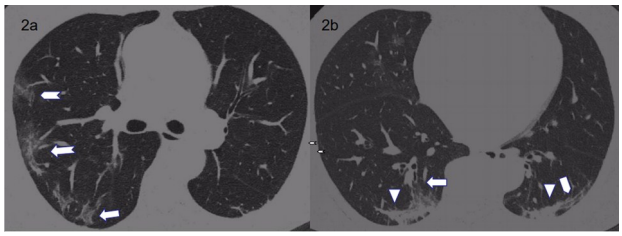

Figure 2. A 63-year-old female patient with nonsevere COVID-19. A CT scan showed multiple patchy pure GGO (⇦), GGO with fine reticulation (⇦) and GGO with focal consolidation (⇦) in the subpleural area of the inferior lobe of the right lung, and the long axis was parallel to the pleural surface **(2a)**. Streak shadows (▽) and patchy consolidation (▽) and GGO with fine reticulation (⇦)were observed in the subpleural area of the inferior lobe of the bilateral lung **(2b)**, and pure GGO in the subpleural area of the middle lobe of right lung **(2b)**.

[DOI: 10.52547/ijrr.20.3.9]

Table 1. Comparison of CT and clinical features of pulmonary lesions between nonsevere and severe COVID-19.

Indicators	States	Nonsevere group number	Severe group number	
Age	≤65y	36	9	χ2=4.401
	>65y	16	12	P=0.036
Sex	male	24	12	χ2=0.723
	female	28	9	P=0.395
Lymphocyte count	normal	43	8	χ2=14.131
	decline	9	13	P<0.001
IL-6	elevate	10	5	χ2=20.118
	normal	40	16	P<0.001
C-reactive protein	elevate	7	12	χ2=13.261
	normal	41	9	P<0.001
Liver function	normal	39	11	χ2=4.681
	abnormal	12	10	P=0.044
Fibrotic appearance	presence	24	16	χ2=5.448
	absence	28	5	P=0.020
Halo sign	presence	1	3	χ2=4.414
	absence	51	18	P=0.020
Reversed halo sign	presence	3	3	χ2=1.438
	absence	49	18	P=0.230
Subpleural line	presence	20	2	χ2=5.950
	absence	32	19	P=0.015
Crazy paving sign	presence	7	13	χ2=17.648
	absence	45	8	P<0.001
Pleural effusion	presence	0	4	P=0.001*
	absence	52	17	
Parallel sign	presence	38	16	χ2=0.075
	absence	14	5	P=0.784
Pure GGO	presence	46	6	χ2=26.184
	absence	6	15	P<0.001
GGO with fine reticulation	presence	45	20	χ2=1.160
	absence	7	1	P=0.281
GGO with focal consolidation	presence	22	16	χ2=6.881
	absence	30	5	P=0.009
Acinar/nodule consolidation	presence	24	12	χ2=0.723
	absence	28	9	P=0.395
Patchy consolidation	presence	20	16	χ2=8.519
	absence	32	5	P=0.004
Sheeted-consolidation	presence	1	7	χ2=15.125
	absence	51	14	P<0.001
CT signs coexistence	GGO+CO	31	18	
	Only GGO	21	2	χ2=8.516 P=0.014
	Only CO	0	1	
Affected lobes	≥3 lobes	41	21	P=0.027*
	<3 lobes	11	0	
Grade of involvement	I grade	29	0	
	II grade	19	4	χ2=43.861
	III grade	4	8	P<0.001
	IV grade	0	9	
Thickened bronchial walls	presence	11	17	χ2=22.623
	absence	41	4	P<0.001
Air bronchi sign	presence	14	14	χ2=9.993
	absence	38	7	P=0.003
Lesions in mid/inner zone	presence	20	19	χ2=16.265
	absence	32	2	P<0.001
Lesions in mid/outer zone	presence	52	21	
	absence	0	0	

* Using Fisher's exact probability method and no χ2 value.
GGO: ground-glass opacity, GGO+CO: GGO plus consolidation, only CO: only consolidation.

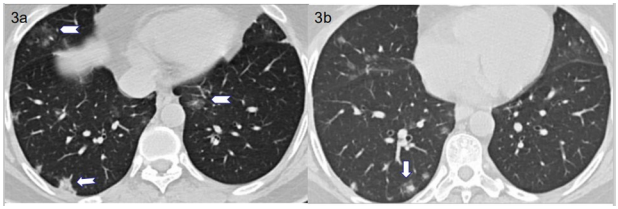

Figure 3. A 48-year-old female patient with nonsevere COVID-19. Patchy consolidation (⇦) was seen in the subpleural area of the right lower lobe **(3a)**, and small patchy pure GGO (⧏) was seen in the lower lobe of the left lung and middle lobe of right lung **(3a)**. Nodular consolidation was demonstrated in the subpleural area of the right lower lobe, surrounded by a small amount of GGO, which formed a so-called halo sign (⇩) **(3b)**.

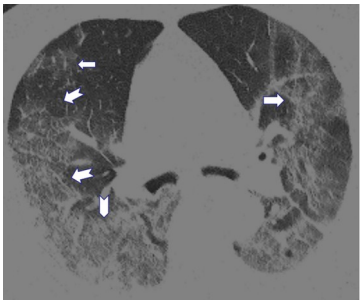

Figure 4. A 75-year-old female patient with severe COVID-19. Diffuse lesions were observed. GGO with fine reticulation (⇦), GGO with focal consolidation (⇩), crazy paving sign (⇦) were visible in the left and right lung.

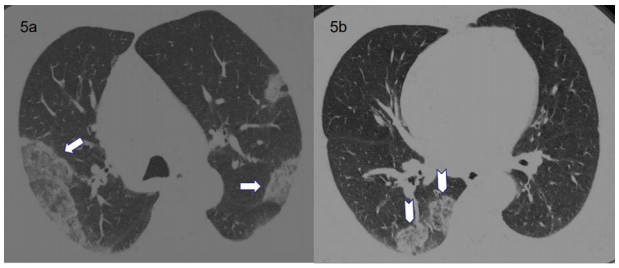

Figure 5. In an 87-year-old male patient with severe COVID-19, a CT scan showed multiple GGO with fine reticulation and GGO with focal consolidation in the subpleural region of both lobes, and the long axis was parallel to the pleural surface **(5a)**. Multiple GGO with consolidation presenting reversed halo signs were demonstrated in the right inferior lobe **(5b)**.

Table 2. Multivariate regression analysis of CT features of COVID-19 lung lesions.

CT features	OR	HR（95% CI）	P value
Pure GGO	30.711	1.292~729.882	0.034
Sheeted consolidation	3.061	0.086~109.023	0.539
Crazy paving sign	0.240	0.020~2.849	0.258
Thickened bronchial walls	0.087	0.006~1.352	0.081
Grade of involvement	0.017	0.001~0.342	0.008
Lesions in mid/inner zone	4.828	0.169~138.184	0.358

GGO: ground-glass opacity, OR:odds ratio, HR:hazard ratio.

[DOI: 10.52547/ijrr.20.3.9]

DISCUSSION

In our data, similar to other studies of COVID-19, the "tree-in-bud" sign, reflecting bronchiolar mucoid impaction occasionally with additional involvement of adjacent alveoli, disappeared [1, 8, 16-18]. Our data showed that different types of GGO were common in lung lesions, especially GGO with fine reticulation. In some studies, COVID-19, whose multifocal intrapulmonary lesions are prone to multileaf involvement, often shows GGO in the peripheral region of the lung, and the appearance of lesions with the long axis parallel to the pleural plane was more common. Presumably, these CT features are related to the fact that 2019-nCoV first destroys angiotensin converting enzyme type 2 receptor of alveolar II epithelial cells when it enters the lungs, which then causes alveolar interstitial inflammation [6,19,20]. GGO may be related to the early formation of a hyaline membrane in the alveolar wall of lung tissue. The pathologic process includes dilatation and congestion of alveolar septal capillaries, leakage of fluid into the alveolar cavity, and edema of interlobular interstitial. Meanwhile, interstitial cell hyperplasia and cellulosic exudation might also be involved in the formation of GGO [1, 8,9,11,16,17].

According to the time after the onset of initial symptoms, Pan et al. divided intrapulmonary lesions into four stages on chest CT: early stage (0-4 days); progressive stage (5-8 days); peak stage (10-13 days); and absorption stage (≥14 days). Early on, it was the main radiological sign that GGO distributed subpleurally [1]. Song *et al.* also found that the most common imaging findings of COVID-19 included pure GGO, GGO with reticulation, and GGO with consolidation. Unfortunately, they did not classify based on the state of illness [11]. However, in our study, GGO with consolidation was common in severe disease, whereas pure GGO was common in no-severe disease, which suggested that alveolar collapse and consolidation in GGO gradually increases with the aggravation of pulmonary diseases. Moreover, the reduction of pure GGO was an independent factor for severe disease. Somewhat inconsistently, in the research of Zhang's team, it was showed that the larger the GGO volume ratio, the worse the prognosis based on AI system [13]. However, they did not carefully distinguish the amount of different types of GGO, and only quantitatively analyzed the volume of GGO, which may be similar to the CT score based on the cumulative lung lobes of the lesion.

Upon further deterioration of the patient, a large area of diffuse alveolar injury with extensive desquamation of pneumocytes and hyaline membrane formation leads to subsequent consolidation and diffuse GGO with a bilateral multilobe distribution [1,11,17,18]. Our research showed that sheeted consolidation emerging in the lung was rare but principally occurred in severe disease. In addition, these patients had a larger range of lung involvement and greater number of involved lobes, which might indicate that pneumonia was more extensive in terms of the pathogenesis of severe disease. Overall, multivariate logistic regression analysis showed that a large area of pulmonary involvement was an independent risk factor for severe disease. These results were similar to Lieveld's team and Zhang's team [12,13]. Compared to patients with nonsevere disease, some with severe disease were more likely to have mild bronchial wall thickening and air bronchograms, which might indicate that with further progression of the disease, the bronchial wall would become mildly affected. Pathological research showed that COVID-19 could cause desquamation necrosis and shedding of the bronchial mucosa without pyogenic infection of the bronchial walls. In addition, the appearance of air bronchograms might be related to the expansion of the lesion into the mid- and inner zones, and the increase in consolidation [21].

A subpleural line sign was considered to be reversible early fibrosis accompanied by alveolar collapse, which is easy to observe in pulmonary interstitial lesions. In our study, we examined the subpleural line sign, which was more common in nonsevere cases. A crazy-paving pattern, considered as thickened interlobular septa and intralobular lines with superimposed ground-glass opacification, was relatively rare in this group [1,16]. However, it was more likely to occur in severe disease, indicating that the interlobular septa might not be the initial main target of damage. Pan et al. found that the crazy-paving pattern appeared in the course of the disease after 5-13 days (progressive stage and peak stage) [1]. The halo sign and reversed halo sign were demonstrated occasionally in COVID-19, which has been frequently reported in association with a variety of conditions, such as cryptogenic organizing pneumonia, fungal inflammation, and tuberculosis [22,23]. However, compared to patients with nonsevere, more halo signs were present in those with severe disease (P=0.020), and we presumed that the halo sign might be a special manifestation of GGO with focal consolidation. Between the two groups, there was a difference in the number of cases with a fibrotic appearance, and we hypothesized that fibrosis might be more pronounced during the development and resolution of intrapulmonary lesions in severe disease. The lack of pleural effusions, noted in our data, was similar with thecharacteristic of SARS and MERS, which are in the same viral family, however, pleural effusions appeared only in patients with severe disease in our data [16,24,25]. In addition, although there was a significant difference in the co-occurrence of CT signs, both the non-severe and severe groups were prone to GGO plus consolidation. On the one hand,

[DOI: 10.52547/ijrr.20.3.9]

perhaps the variations in pathology, reflected by coexistence of CT signs, were due to coinstantaneous damage of parenchyma and stroma [11,26,27]. On the other hand, as described above, consolidation was more likely to occur in severe cases. There were more patients with abnormal laboratory results in the severe group, including increases in IL-6 and C-reactive protein levels, abnormalities in liver function, and lymphopenia [5].

Perhaps in clinical practice, the development mode of the disease cannot be predicted, and patients undergoing dynamic CT examination may face the risk of large doses of radiation damage and hospital exposure. More importantly, medical resources are scarce in the face of the epidemic. In view of these limitations, we did not plan reexamination by CT based on a strict timeline and clinical symptoms, and one of our study limitations was that the analysis of correlations between the dynamic changes in clinical conditions and CT signs was not implemented.

CONCLUSIONS

In summary, patients who suffer from COVID-19 have diverse CT features of intrapulmonary lesions, but still have some characteristics. On admission, some CT findings would serve as a potential alert in the management of patients with severe disease, such as inadequate pure GGO, high degree of GGO with focal consolidation and patchy or sheeted consolidation, more intrapulmonary lesions located in the mid/inner zone, a large area of lung involvement, the appearance of pleural effusion and crazy-paving patterns, and bronchial wall thickening. In particular, a lack of pure GGO and extensive damage on CT may be independent risk factors for patients with severe disease.

ACKNOWLEDGEMENTS

The authors would like to express their appreciation for all of the emergency services, nurses, doctors, and other hospital staff for their efforts to combat the COVID-19 outbreat.

***Ethical approval*:** All procedures performed in studies involving human participants were in accordance with the 901st Hospital of the Joint Logistic Support Force of People's Liberation Army (PLA) Ethics Committee (certificate No. 2020030102) and with the 1964 Helsinki Declaration and its later amendments or comparable ethical standards.

***Author contributions*:** All authors contributed to the study conception and design. Qian Zhang and Zi Mo acquired the data and drafted the manuscript. Zi Mo, Xiang-wei Luo, Qian Zhang, Tian qin, You-zhi Zhu and Yu Zhang analyzed and interpreted the data and performed statistical analysis. Xiang-wei Luo and Yu Zhang reviewed the manuscript, figures and tables. All authors read and approved the final manuscript.

***Conflict of Interest*:** The authors declare that they have no conflict of interest.

REFERENCES

1. Pan F, Ye T, Sun P, Gui S, Liang B, Li L, *et al.* (2020) Time Course of Lung Changes on Chest CT During Recovery From 2019 Novel Coronavirus (COVID-19) Pneumonia. *Radiology,* ***295****(3): 715-721*.
2. Coronaviridae Study Group of the International Committee on Taxonomy of Viruses (2020) The species Severe acute respiratory syndrome-related coronavirus: classifying 2019-nCoV and naming it SARS-CoV-2. *Nat Microbiol,* ***5****(4): 536–544*.
3. Jiang S, Shi Z, Shu Y, Song J, Gao GF, Tan W, *et al.* (2020) A distinct name is needed for the new coronavirus. *Lancet,* ***395****(10228): 949*.
4. Wu Z and McGoogan JM (2020) Characteristics of and important lessons from the coronavirus disease 2019 (COVID-19) Outbreak in China: Summary of a Report of 72 314 Cases From the Chinese Center for Disease Control and Prevention. *JAMA,* ***323****(13): 1239-1242*.
5. Guan WJ, Ni ZY, Hu Y, Liang WH, Ou CQ, He JX, *et al.* (2020) Clinical Characteristics of Coronavirus Disease 2019 in China. *N Engl J Med,* ***382****(18): 1708–1720*.
6. Lu R, Zhao X, Li J, Niu P, Yang B, Wu H, *et al*. (2020) Genomic characterisation and epidemiology of 2019 novel coronavirus: implications for virus origins and receptor binding. *Lancet,* ***395****(10224): 565–574*.
7. Yu WB, Tang GD, Zhang L, Corlett RT (2020) Decoding the evolution and transmissions of the novel pneumonia coronavirus (SARS-CoV-2 / HCoV-19) using whole genomic data. *Zool Res,* ***41****(3): 247-257*.
8. He X, Zheng J, Ren J, Zheng G, Liu L (2020) Chest high-resolution computed tomography imaging findings of coronavirus disease 2019 (Covid-19) pneumonia. *Int J Radiat Res,* ***18****(2): 343-349*.
9. Ai T, Yang Z, Hou H, Zhan C, Chen C, Lv W, *et al.* (2020) Correlation of Chest CT and RT-PCR Testing in Coronavirus Disease 2019 (COVID-19) in China: A Report of 1014 Cases. *Radiology,* ***296****(2): E32-E40*.
10. Wang YXJ, Liu WH, Yang M, Chen W (2020) The role of CT for Covid-19 patient's management remains poorly defined. *Ann Transl Med,* ***8****(4): 145*.
11. Song F, Shi N, Shan F, Zhang Z, Shen J, Lu H, *et al.* (2020) Emerging 2019 Novel Coronavirus (2019-nCoV) Pneumonia. *Radiology,* ***295*** *(1): 210-217*.
12. Lieveld AWE, Azijli K, Teunissen BP, van Haaften RM, Kootte RS, van den Berk IAH, *et al.* (2021) Chest CT in COVID-19 at the ED: Validation of the COVID-19 Reporting and Data System (CO-RADS) and CT severity score: a prospective, multicenter, observational study. *Chest,* ***159****(3):1126-1135*.
13. Zhang K, Liu X, Shen J, Li Z, Sang Y, Wu X, *et al*. (2020) Clinically applicable Ai system for accurate diagnosis, quantitative measurements, and prognosis of COVID-19 pneumonia using computed tomography. *Cell,* ***182****(5): 1360*.
14. Metlay JP, Waterer GW, Long AC, Anzueto A, Brozek J, Crothers K, *et al.* (2019) Diagnosis and Treatment of Adults with Community-acquired Pneumonia. An Official Clinical Practice Guideline of the American Thoracic Society and Infectious Diseases Society of America. *Am J Respir Crit Care Med,* ***200****(7): e45–e67*.
15. Hansell DM, Bankier AA, MacMahon H, McLoud TC, Müller NL, Remy J (2008) Fleischner Society: glossary of terms for thoracic imaging. *Radiology,* ***246****(3): 697-722*.
16. Chung M, Bernheim A, Mei X, Zhang N, Huang M, Zeng X, *et al.* (2020) CT Imaging Features of 2019 Novel Coronavirus (2019-nCoV). *Radiology,* ***295****(1): 202–207*.
17. Jin YH, Cai L, Cheng ZS, Cheng H, Deng T, Fan YP, *et al.* (2020)A rapid advice guideline for the diagnosis and treatment of 2019 novel coronavirus (2019-nCoV) infected pneumonia (standard version). *Mil Med Res,* ***7****(1): 4*.
18. Pan Y, Guan H, Zhou S, Wang Y, Li Q, Zhu T, *et al.* (2020) Initial CT findings and temporal changes in patients with the novel coronavirus pneumonia (2019-nCoV): a study of 63 patients in Wuhan, China. *Eur Radiol,* ***30****(6): 3306-3309*.
19. Cheng ZJ and Shan J (2020) 2019 Novel coronavirus: where we are and what we know. *Infection,* ***48****(2): 155-163*.
20. Tian S, Hu W, Niu L, Liu H, Xu H, Xiao SY (2020) Pulmonary pathol-

[DOI: 10.52547/ijrr.20.3.9]

ogy of Early-phase (2020) 2019 novel coronavirus (COVID-19) Pneumonia in Two Patients With Lung Cancer. *J Thorac Oncol,* ***15*** *(5): 700-704*.
21. Xu Z, Shi L, Wang Y, Zhang J, Huang L, Zhang C, *et al.* (2020) Pathological findings of COVID-19 associated with acute respiratory distress syndrome. *Lancet Respir Med,* ***8****(4): 420-422*.
22. Alves GR, Marchiori E, Irion K, Nin CS, Watte G, Pasqualotto AC, *et al.* (2016) The halo sign: HRCT findings in 85 patients. *J Bras Pneumol,* ***42****(6): 435-439*.
23. Godoy MC, Viswanathan C, Marchiori E, Truong MT, Benveniste MF, Rossi S, *et al.* (2012) The reversed halo sign: update and differential diagnosis. *Br J Radiol,* ***85****(1017): 1226–1235*.
24. Ooi GC and Daqing M (2003) SARS: radiological features. *Respirology,* ***8****(1): S15-9*.
25. Ajlan AM, Ahyad RA, Jamjoom LG, Alharthy A, Madani TA (2014) Middle East respiratory syndrome coronavirus (MERS-CoV) infection: chest CT findings. *AJR Am J Roentgenol,* ***203****(4): 782-787*.
26. Bradley BT and Bryan A (2019) Emerging respiratory infections: The infectious disease pathology of SARS, MERS, pandemic influenza, and Legionella. *Semin Diagn Pathol,* ***36****(3): 152–159*.
27. Liu J, Zheng X, Tong Q, Li W, Wang B, Sutter K, *et al.* (2020) Overlapping and discrete aspects of the pathology and pathogenesis of the emerging human pathogenic coronaviruses SARS-CoV, MERS-CoV, and 2019-nCoV. *J Med Virol,* ***92****(5): 491–494*.

[DOI: 10.52547/ijrr.20.3.9]